

Morpho-Quantitative Stereological Analysis of Peripheral and Optic Nerve Fibers

Stefano Geuna, Sefania Raimondo, Michele Fornaro,
Maria Giuseppina Robecchi

ABSTRACT

Morpho-quantitative stereological assessment of nerve fibers is a main research task in various biomedical disciplines, including neuroanatomy, neuropathology, neurosurgery and reconstructive microsurgery. In this paper, we will critically outline the modern approaches for nerve fiber quantitative assessment based on design-based 2D stereology and describe the principal morphological indicators of function loss and recovery that can be quantitatively assessed. Yet, the pros and cons of the main morphological techniques for investigating the structure and ultrastructure of axons in the peripheral nerves as well as in the optic nerve are given in appendix. This paper is directed towards all those basic and clinical researchers who wish to undertake the histomorphometrical study of peripheral and optic nerve in choosing the best morphological methods to meet their scientific goals.

Key Words: peripheral nerve fibers, optic nerve, nerve regeneration, 2D-design-based stereology, osmium tetroxide, light microscopy, electron microscopy

NeuroQuantology 2012; 1: 95-105

Introduction

The study of the morphology of nerve fibers is one of the pillars for the investigation of peripheral and optic nerves in various physiological, pathological and experimental conditions (Vleggeert-Lankamp, 2007).

For example, nerve fibers morphology can give us important information on the time course of axon growth and maturation during development (Canan *et al.*, 2008) as well on the age-related nerve fiber changes (Clavijo-Alvarez *et al.*, 2007). Yet, the prognosis of a number of diseases and the efficacy of a treatment against them can be assessed by structural and ultrastructural analysis of the nerves and several morphological indicators of axonal regeneration can tell us about the extent a nerve trauma and the effectiveness of

microsurgical and tissue engineering techniques to repair it (Lundborg, 2005; Geuna *et al.*, 2004a;2006;2007; Luis *et al.*, 2007; Papalia *et al.*, 2003;2007; Roglio *et al.*, 2008; Siniset *et al.*, 2006;2007;2008; Acaret *et al.*, 2008; Raimondo *et al.*, 2011).

In fact, although in the clinical perspective functional assessment is always the key element in the assessment of the nervous system, nonetheless the correlation of some morphological features with nerve function have been demonstrated (Kanaya *et al.* 1996), thus strengthening the importance of the morpho-quantitative assessment in the context of experimental and clinical nerve studies (Vleggeert-Lankamp, 2007).

Although nerves located in the various part of the body differs with respect to the fiber type composition and the presence and number of fascicles, their morphology is relatively similar in all districts (Lundborg, 2005; Geuna *et al.*, 2009). The only two nerves the structure of which is completely different in comparison to all other nerves are the first two cranial nerves, namely olfactory and optic

Corresponding author: Stefano Geuna

Address: Neuroscience Institute of the "Cavalieri Ottolenghi" Foundation & Department of Clinical and Biological Sciences, University of Turin, Regione Gonzole 10, Orbassano (TO), Italy.
Phone: +39.011.90.38.639

✉stefano.geuna@unito.it

Received July 17, 2011. Revised Sept 11, 2011. Accepted Jan 2, 2012



nerves. Olfactory nerve is composed of very small unmyelinated axons originating from olfactory sensory neurons located peripherally in the nasal cavity (a unique feature among peripheral nerves) and grouped to form about 20 branches that pass back through the cribriform plate into the olfactory bulb (Williams, 1999). The peculiarity of this nerve fascicles is that they are continuously regenerated throughout life due to the continuous turnover in the neuron population of the olfactory mucosa. Optic nerve is composed of small myelinated axons originating from multipolar (ganglion) neurons in the retina. Optic nerves (like retina) are unique in their being outgrowths of the brain and covered by oligodendrocytes (and not Schwann cells like all other peripheral nerves). Therefore, in spite of their peripheral location they have to be considered part of the central nervous system (Williams, 1999).

The aim of this paper is to describe the main morphological indicators of nerve function loss and recovery together with the modern approaches for their quantitative assessment by design-based 2D stereology. In addition, the main morphological techniques for investigating the structure and ultrastructure of axons in both peripheral nerves as well as in the optic nerve are also given in appendix.

Quantitative parameters of nerve fibers

The most important geometrical parameters that can be used for the assessment nerve fibers are table in **Table 1**.

Table 1. Quantitative parameters for myelinated nerve fiber assessment

1. Number of fibers
2. Density of fibers
3. Diameter of fibers and axons (Maximum, Minimum, Circle-equivalent)
4. Cross-sectional area of fibers and axons
5. Perimeter of fibers and axons
6. Myelin thickness
7. Myelin-thickness/axon-diameter ratio
8. Fiber-diameter/axon-diameter ratio or axon-diameter/fiber-diameter (g-ratio)

The number and density of nerve fibers is the main parameter that is evaluated in nerve research. Changes in the number of nerve fibers (especially myelinated ones) are important for the investigation of the effects of

various pathological conditions on the nerve structure, such as and mercury intoxication (Schionning and Larsen, 1997) and zinc deficiency (Unalet *al.*, 2005). Moreover, fiber number is one of the key indicators in those experimental studies that investigate the efficacy of microsurgical and tissue engineering techniques for the reconstruction of severed peripheral nerves (Keskinet *al.*, 2004; Amado *et al.*, 2008).

Fiber and axon diameter, together with the conduction velocity, is the classical parameter for nerve type identification since it has proved to be the main determinant of conduction velocity (Hoffman, 1995). Various types of diameters of nerve fibers and/or axons have been used to assess their size (Geunaet *al.*, 2001): the maximum diameter (which is strongly biased by obliquity of cross-sectional fiber profiles), the minimum diameter (which is strongly biased by fiber shrinkage), and the circle-equivalent diameter (which represents the diameter of a circle the area of which corresponds to the cross-sectional area of the fiber and/or axon). Cross-sectional area is another commonly used size estimation parameter for myelinated nerve fibers. However, data on the cross-sectional area of nerve fibers are less easy to be interpreted by readers, in comparison with diameter data, classical parameter used to classify nerve fibers (Hoffman, 1995) and thus the use of diameter is to be preferred for indicating nerve fiber and axon size (Geunaet *al.*, 2001).

Using data fiber and axon size, several other size parameters can be achievable by simple mathematical calculations. The most used are: myelin thickness, the myelin-thickness/axon-diameter ratio; the fiber-diameter/axon-diameter ratio and its opposite, the axon-diameter / fiber-diameter ratio (g-ratio). These parameters are particularly important for the investigation of nerve development (Fraheret *al.*, 1990) or regeneration (Kanayaet *al.*, 1996).

The final decision on the selection of the size parameters should represent one of the main steps of the study-design and should be done on the basis of the quality of the histological material, the equipment available and, eventually, the demands of the quantitative data that are sought.

Potential sources of bias in quantitative assessment of nerve fibers

Possible foundations of bias can exist at various levels in the quantitative assessment of nerve fibers (Geuna *et al.*, 2001).

Level 1. The strain, gender and age of experimental animals (strain-related, gender-related, age-related foundations of bias).

Level 2. The point (level) along the nerve axis where sections are cut (section-related foundations of bias).

Level 3. The location of the sampling fields within the nerve cross-section profile (location-related foundations of bias).

Level 4. The inclusion-exclusion rules for sampling fiber profiles within the sampling fields (morphology-related foundations of bias).

Level 5. The method for measuring the selected size parameters (measurement-related foundations bias).

The first two potential level of bias are related to the study design, while levels 2, 3 and 4 are related to the sampling procedure and the method used for quantitative nerve fiber assessment. Therefore, in the following paragraphs we will focus on the latter issues describing, in particular, the basic principles and methods for design-based sampling and for nerve fiber stereology.

Design-based sampling and stereological assessment of nerve fibers

The methods for the quantitative assessment of tissue and organs on histological section have been the subject of heated scientific debate over the past 20 years in parallel with the emergence of an innovative group of techniques popularly known as *stereology*. In particular, stereological techniques have represented a significant innovation in neuromorphology, providing scientists with specific tools designed to solve particular problems that could not be properly addressed before, such as the estimation of neocortical neuron number in humans (Pakkenberg and Gundersen, 1997). A comprehensive critical evaluation of stereological advancements can be found in several article including Mayhew and Gundersen (1996), West (1999), Geuna (2000, 2005), Benes and Lange (2001); Guillery (2002), von Bartheld (2002), Schmitz and Hof (2005), Baryshnikova *et al.* (2006), and Canan *et al.* (2008).

As regards nerve fiber quantitative assessment using stereological methods, only few papers have addressed this issue. In particular, two method have been the most employed so far: the unbiased sampling frame (Gundersen, 1978; Larsen, 1998; Keskinet *et al.*, 2004; Acaret *et al.*, 2008; Canan *et al.*, 2008; Kaplan *et al.*, 2010) and the 2D disector (Gundersen, 1986; Geuna *et al.* 2000, 2001; Raimondo *et al.*, 2009; Kaplan *et al.*, 2010).

Selection of sampling fields: Systematic random sampling

The “golden rule” of sampling for any tissue and organ is the equal opportunity rule (Cruz-Orive and Weibel, 1981). This means that all objects must have the same opportunity of being included in the sample! The basic sampling paradigm that is usually employed to respect the equal opportunity rule is called design-based sampling where the term design refers to a system of sampling rules designed such that all objects in the sampling space have the same probability of being sampled (Geuna, 2000). Since the final goal of design-based sampling is to reach randomness, design-based sampling can also be referred to as random sampling.

Simple random sampling is the most basic random-based design and provides that all possible combinations of n sampling units have the same probability of being selected from among the total N sampling units in the population. This sampling design requires a high amount of sampling to obtain a sufficient estimate precision and is impossible in histology as it would require the specimen to be glued together and re-sectioned after each section was selected (Geuna, 2000).

Other random sampling designs include systematic, multistage, and stratified random sampling (Cochran, 1977). Systematic random sampling is the systematic selection of every n^{th} unit of the population from one randomly selected starting unit (where n is the distance between units that is decided in relation to the amount of sampling required). In multistage random sampling, primary sample units are first selected, and then secondary sample units are selected within each primary unit. Finally, in stratified random sampling, the population is subdivided into strata, and each stratum is sampled separately.

Systematic random sampling appears to be the most adequate in nerve fiber stereology, as well as in most other neuromorphological application. The units are the single sampling boxes on a given nerve cross-section, and, after the starting box is selected by chance, the following boxes are selected by systematically jumping at a given distance from the former box.

Inclusion and exclusion rules: the edge effect

Once the sampling fields are selected within the nerve cross section by systematic random sampling (fig. 1), it is necessary to define a set of inclusion/exclusion rules for clearly determining which nerve fiber falls inside the sampling field, and which other does not (Geunaet *al.*, 2004b). The bias originating from an unclear determination of inclusion/exclusion rules depends on the so-called “edge effect” (Gundersen, 1977). This is mainly due to variability in the morphology of nerve fiber profiles (especially in their size) which may cause significant differences in the probability of each profile being intersected by the sampling frame edges and appearing in more than one sampling field: larger fibers will have a higher probability of intersecting the frame edges and thus of partially falling into more than one sampling field than smaller fibers. If all edging fiber profiles are included, quantitative estimations will be biased towards a systematic overestimation of number and size of fibers, while if all edging fiber profiles are excluded from sampling, quantitative estimations will be biased toward a systematic underestimation of fiber number and size.

Unfortunately, most published papers including data on nerve histomorphometry do not provide any information on “what happens” when a fiber profile intersects the histological field edges and it is thus not possible to know if this edge effect-related bias was avoided.

In order to cope with the edge effect, researchers have to respect the “equal opportunity rule” which is based on the adoption of a set of inclusion/exclusion rules that assures that any profile of nerve fiber has the same chance of being sampled, independently of its size, shape and orientation, i.e. independently of the number of edge intersections.

As already mentioned, two are the most used stereological methods that have been used so far for coping with the edge effect: the unbiased sampling frame and the 2D disector.

Unbiased sampling frame

This method was first described by Gundersen (1978) and has been applied to several stereological studies on peripheral nerve fibers (Larsen, 1998; Keskinet *al.*, 2004; Acaret *al.*, 2008; Canan *et al.*, 2008). The method is based on the employment of a squared counting frame in which two edges are exclusion (forbidden) lines: when an axon touches to these lines (including their infinite extension) is excluded from the counting. By contrast, the other two edges of the frame are called inclusion lines and when an axon touches them, it is included to counting. When an axon touches both an inclusion and an exclusion line, the former prevails an axon is thus excluded. In order to have the possibility to assess also the extensions of the square edges (especially the forbidden lines), it is necessary to use sampling frames that are smaller than the whole monitor/printed area in order to permit the inspection of the “guard area” around each counting frame.

Two-dimensional (2D) disector

The two dimensional disector is an adaptation of the disector principle (that is used for sampling object in 3D) and it is basically an associated-point method, i.e. a method based on the identification of an “univocal” reference point in each particle (the “top”) and then the inclusion of the particle in the sampling frame only if this point falls inside the frame independently from what happens to the rest of the particle (Geuna, 2000;2005; Raimondoet *al.*, 2009). In the 2D disector, the “top” is identified as the “higher” edge of a fiber profile and thus nerve fibers are considered inside the frame, and thus counted; only when their “top” falls inside the box borders (**Fig. 1**). Whereas, the first description of the 2D-disector (Geunaet *al.*, 2000) was based on the employment of a squared frame, we currently prefer to use a circular frame in order to reduce the probability of nerve fibers (that have a circular shape) to hit the frame border (Raimondoet *al.*, 2009). When a fiber’s top exactly falls on the line (**Fig.1**), an inclusion hemi circle (the higher dashed green one) and an exclusion hemi circle (the lower red solid one) are adopted (when the top a

fiber touches the lower hemi circle is excluded from counting and vice versa).

Discussion

Nerve research is receiving increasing interest in biomedicine for the many biological and clinical issues related to this very peculiar organ (Lundborg, 2002; Toset *et al.*, 2004; Chalfoun, 2006; Geunaet *al.*, 2003; 2006; Hoke, 2006; Chen *et al.*, 2007; Roglioet *al.*, 2007; Campbell, 2008; Raimondoet *al.*, 2011; Kaplan *et al.*, 2011). In this context, assessment of peripheral nerve morphology is a very important element for assessing, both qualitatively and quantitatively, the damage and regeneration of nerve fibers in various pathological and experimental conditions (Vleggeert-Lankamp, 2007).

In this paper we critically addressed the methods for the quantitative assessment by design-based 2D stereology of nerve fibers and it should be pointed out that the stereological approach to quantitative morphology has raised a lively debate among researchers over the last twenty years (Saper, 1999; Benes and Lange 2001; Guillery 2002, Von Bartheld 2002; Gardellaet *al.*, 2003; Baryshnikovaet *al.*, 2006; Ward *et al.*, 2008; Kaplan *et al.*, 2010). Luckily, the basic concepts of design-based stereology are becoming progressively better known due to the increasing number of instructional courses that hare being carried out worldwide as well as the inclusion of stereological softwares in several commercially available integrated PC systems for quantitative morphology. Unfortunately, in spite increase in the number of papers reporting quantitative data on peripheral nerve fibers due to the increasing clinical importance of peripheral nerve injury and disease and their treatment (Chen *et al.*, 2007; Vleggeert-Lankamp, 2007; Campbell, 2008), most studies on peripheral nerve quantitative morphology are based on weak histomorphometrical methods that are not designed to cope with the several potential sources of bias outlined in this paper. This paper is thus directed towards all those researchers who seek for quantitative results on peripheral nerve fibers, but who have little or no knowledge on the issues of sampling and bias, as well as toward readers of papers reporting quantitative data on nerve fiber in order to provide them with the basic

information for a critical assessment on the significance and reliability of published results.

In any case, we shall always keep in mind that stereological methods should not be aprioristically considered superior to all other methods and that there is no absolutely correct method for solving any problem that involves inductive reasoning (Smith, 1994; Geuna, 2005). Any method should be critically evaluated by researchers in order to verify its appropriateness, identify its limitations, and interpret the results within those limitations. It is hoped that this critical and informed approach, shared by researchers with different scientific backgrounds, will lead to an improvement in the quality of results obtained in nerve studies and thus in the usefulness of these results in the perspective of improving patient's outcome after nerve damage.

APENDIX I

Protocols for nerve fixation and embedding

Nerve sample fixation is peculiar in comparison to most other organs. In fact, while good structural, and especially ultrastructural, fixation of most organs requires intracardiac perfusion only, in the case of nerves fixation by immediate immersion in the paraformaldehyde or glutaraldehyde solution is sufficient to guarantee the good preservation of the histological and cytological features of axons, glial cells and the other nerve elements.

Yet, this type of immersion fixation procedure should even be preferred to perfusion fixation because it enables to researcher to keep the nerve segment in a straight position during earlier instants of fixation. The specimen will then maintain the straight shape until embedding and this represents a significant technical advantage for permitting the adequate orientation during sectioning.

For light microscopy observation, nerve specimens can be processed were processed either with paraformaldehyde fixation followed by paraffin, or with glutaraldehyde fixation and osmium/tetroxide postfixation followed by resin embedding. Although the latter procedure is the far most used for nerve

fiber analysis (Di Scipio *et al.*, 2008), in the following paragraph we will describe both protocols since we have recently shown that, the addition of osmium/tetroxide postfixation to the traditional protocols for paraffin embedding leads to very good nerve fiber imaging and represents thus a good alternative to resin embedding (Di Scipio *et al.*, 2008).

Paraformaldehyde fixation and paraffin embedding

Nerve samples are fixed in 4% paraformaldehyde (Fluka, Buchs, Switzerland) in PBS (Phosphate Buffered Saline) for 2-4 h and then washed and stored in 0.2 g glycine in 100 ml PBS. Following dehydration with ascending ethanol passages (50%, 80%, 95%, 100%) and diaphanization in Xylol or similar products such as Bioclear (Bio-Optica, Milano, Italy), the specimens are embedded in paraffin. In alternative, nerves could also be embedded in ice, or OCT medium, but this procedure is only occasionally used in our laboratory since most antibodies useful for assessing nerve fibers can be employed on paraffin-embedded sections.

We have recently shown that the histological quality of axons on paraffin-embedded nerve sections can be strongly ameliorated by the addition of osmium tetroxide post-fixation before embedding because of its excellent properties as myelin sheath stain (Di Scipio *et al.*, 2008). After paraformaldehyde fixation and PBS storage, on the day of embedding, the nerves are first washed in fresh PBS again for few minutes and then immersed in 2% osmium tetroxide (Sigma, St. Louis, MO), in the same PBS solution, for 2h. Then, nerves are dehydrated by an increasing alcohol series, starting from 30% ethanol, with numerous passages, as in the procedure commonly used for dehydration before resin embedding. The specimens are finally embedded in paraffin (or ice) as described above.

Paraffin and ice block are usually cut transversely to the main nerve axis and with a nominal thickness ranging from 5µm to 10µm. Longitudinal sections are more technically challenging and are thus usually not cut for nerve analysis. One exception is immunofluorescence analysis of regenerating axons after nerve damage and repair which, when performed on longitudinal nerve sections, permits to measure the length of

growing axons and thus gives important information on the quickness of the regeneration process. We use a RM2135 microtome from Leica Microsystems (Wetzlar, Germany).

After cutting, sections are positioned on slides and usually put into a drying oven overnight to obtain an optimal distension of tissue slices.

Glutaraldehyde fixation and resin embedding

Nerve samples are fixed in a solution of 2.5% purified glutaraldehyde (Histo-line Laboratories s.r.l., Milano, Italy) and 0.5% saccarose (Merck, Darmstadt, Germany) in 0.1M Sörensen phosphate buffer, pH 7.4, for 6-8h. Specimens are then washed and stored in 1.5% saccarose in 0.1M Sörensen phosphate buffer at 4-6°C. Sörensen phosphate buffer comprises 56 g di-potassium hydrogen phosphate 3-hydrate ($K_2HPO_4 \cdot 3H_2O$) (Fluka, Buchs, Switzerland) and 10.6 g sodium di-hydrogen phosphate 1-hydrate ($NaH_2PO_4 \cdot H_2O$) (Merck, Darmstadt, Germany) in 1,000 ml doubly-distilled water.

Prior to embedding (in our experience, the nerves can be stored for several, days or even weeks, in Sörensen phosphate buffer at 4-6°C after glutaraldehyde fixation), the nerves are washed in 1.5% saccarose in 0.1M Sorensen phosphate buffer for a few minutes and then immersed for 2 h in 2% osmium tetroxide (Sigma, St.Louis, MO) in the same buffer solution (see paragraph 2.1.3 for more information on the safety procedures for handling osmium tetroxide).

The specimens are then dehydrated with numerous alcohol passages (starting from 30%) and embedded in Glauerts' embedding mixture of resins, comprising equal parts of Araldite M and the Araldite Härter, HY 964 (Merck, Darmstad, Germany), to which 2% of accelerator 964, DY 064 is added (Merck, Darmstad, Germany). The plasticizer dibutylphthalate was added to 0.5%.

Resin blocks can be cut, usually transversely to the main nerve axis, both as semi-thin sections for light microscope observation, with a thickness ranging from 0.5µm to 2.5µm (we usually cut nerves at 2-2.5µm in order to have a more tissue in each section) and as ultra-thin sections for electron microscope observation (with a nominal

thickness ranging from 50nm to 75nm). Both semi-thin and ultra-thin cutting is usually carried out by an ultramicrotome (we use an Ultracut UCT microtome from Leica Microsystems, Wetzlar, Germany).

For electron microscope analysis glutaraldehyde fixation before osmium tetroxide post-fixation and resin embedding are required for preserving the ultrastructural features of the nerve fibers. In particular, inadequate fixation (e.g. by paraphormaldehyde only) leads to ultrastructural artefacts, especially evident on the myelin sheaths in the forms of swelling and disorganization of the lamellae which might be confused with myelin damage.

Since ultra-thin sections are usually cut by ultramicrotome using the same resin-embedded blocks used for preparing semithin sections, it is possible to use light microscopy observations to orientate ultrastructural examination on the most preserved parts of the nerve.

The role of pre-embedding osmium tetroxide post fixation/staining and safety procedures for using osmium tetroxide

Since it is well known that the gold standard for light microscopic imaging of myelinated nerve fibers is toluidine blue staining of resin-embedded semithin sections, many researchers are unaware that the dark staining of myelin sheaths typically produced by this procedure is due to osmium tetroxide post-fixation and not to toluidine blue. We have recently described (Di Scipio *et al.*, 2008) a simple pre-embedding protocol for staining myelin sheaths in paraffin-embedded nerve specimens using osmium tetroxide (see paragraph 2.1.1) which represents a valid alternative to the conventional resin embedding-based protocol: it is much cheaper, can be adopted by any histological laboratory and allows immunohistochemical analysis to be conducted (Di Scipio *et al.*, 2008).

The only disadvantage of this procedure is that toxicity of osmium tetroxide is high and thus safety procedures for handling this chemical have to be carefully and strictly respected. Osmium tetroxide is a strong oxidant. It has a high vapour pressure and should not be inhaled or allowed to contact the skin. Osmium solutions (usually sold as 2% or 4%) should be stored double-bottled (to avoid

vapour dispersion) in a refrigerator restricted to specialized personnel only. Handling of this chemical should also be carried out by expert personnel only and all post-fixation steps should be carried out under a chemical fume hood. Alcohol washes of specimens after osmium immersion must be numerous (3 to 5 passages for each ethanol concentration). They must be carried out under a chemical fume hood and waste must be treated as osmium tetroxide solutions, i.e. collected by specialized waste disposal personnel after being placed in properly labelled containers. If osmium solution turns black (i.e. osmium's reduction occurred because of contamination), it must be eliminated.

APPENDIX II

Protocols for nerve fiber staining

Light microscopy

Three main staining techniques can be used for staining of nerves: haematoxylin and eosin and Masson's trichrome (on paraffin sections), and toluidine blue (on resin sections). While the three techniques used alone do not provide a satisfactory imaging of nerve fibers, the addition of pre-embedding osmium tetroxide leads to much better results for the reasons outlined before and thus should always be carried out.

For haematoxylin and eosin staining, slides are deparaffinated, rehydrated with decreasing ethanol passages and immersed in 0.1% haematoxylin (Ciba, Basle, Switzerland) for 10 min. Slides are then washed in tap water for 15 min and immersed in 0.1% eosin (Ciba, Basle, Switzerland) for 5 min. Slides are finally washed in distilled water, dehydrated and mounted in DPX (Fluka, Buchs, Switzerland).

For Masson's trichrome staining, in our laboratory we adopted a "Masson trichrome with aniline blue" kit from Bio-Optica (Milano, Italy). After deparaffination and rehydration, six drops of Weigert's iron haematoxylin (solution A) and 6 drops of Weigert's iron haematoxylin (solution B) are put on the sections and left to act for 10 min. Then, without washing, the slides are drained and 10 drops of alcoholic picric acid solution are added to the sections for 4 min. After washing quickly in distilled water, 10 drops of Ponceau acid fuchsin are added, left to act for 4 min and washed again in distilled water. Then 10

drops of phosphomolybdic acid solution are added and left to act for 10 min. Without washing, the slides are drained and 10 drops of aniline blue were added for 5 min. Finally, after washing in distilled water, dehydrating rapidly and clearing with Bioclear (Bio-Optica, Milano, Italy), the slides are mounted in DPX (Fluka, Buchs, Switzerland).

For toluidine blue staining of semithin sections of resin-embedded blocks, semi-thin transverse sections 2-3 μ m thick are cut using a ultramicrotome (we use a Leica Ultracut UCT, Leica Microsystems, Wetzlar, Germany) and stained with 1% Toluidine blue (Fluka, Buchs, Switzerland) on a 60°C hot plate for 30-45s.

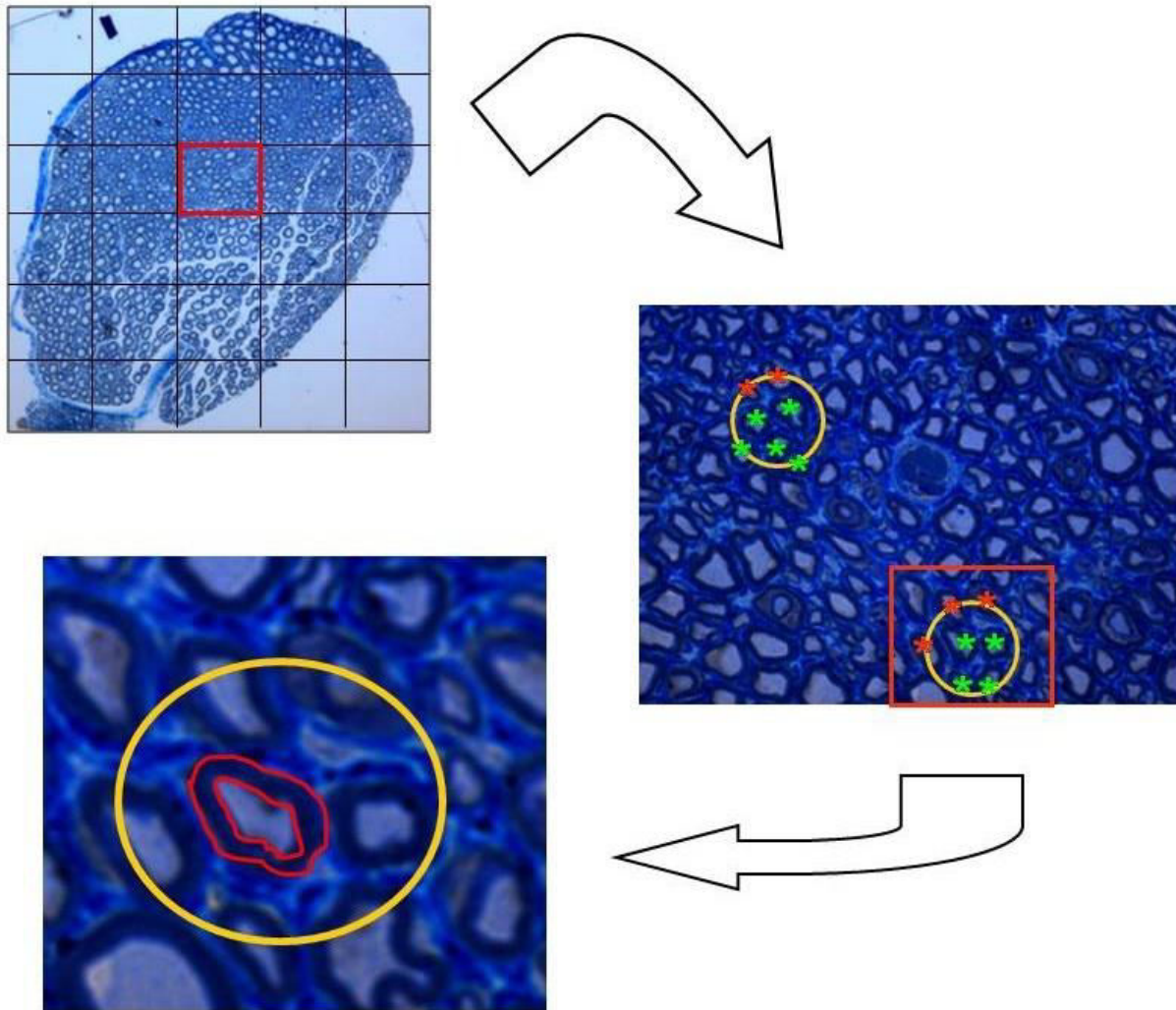


Figure 1. The three steps of design-based stereology of nerve fibers. First (upper left picture), systematic random sampling of evaluation nerve fields. Second (right picture), 2D-disector sampling of nerve fibers inside each sampling field. Third (lower left picture), axon, fiber and myelin sheath measurement of each sampled nerve fiber.

Immunofluorescence and confocal microscopy

Immunohistochemistry (especially immunofluorescence followed by laser confocal imaging) has gained more and more importance in nerve research and, today, many good antibodies are available for detecting various nerve tissue antigens. Among the variety of antibodies, the most used are those, which permit to mark the two main components of the nerves, namely axons and

Schwann cells (Raimondoet *al.*, 2005). For the former, a-neurofilament antibodies are those, which are most used and permit to trace axons (even small ones) in both transverse and longitudinal sections. As concerns Schwann cell markers, the most used is S-100 since it labels most glials cells in the nerve, though it should be noted that Schwann cells may lose their S100 positivity during nerve damage and regeneration when they shift from an adult to a less differentiated phenotype which can be

better identifiable by GFAP (glial fibrillar acid protein).

While in general cryosections are better for immunofluorescence, in nerves we usually obtain excellent results also working on paraffin-embedded samples (in case of excessive fluorescent background, few minutes of microwave etching of slides is sufficient to eliminate it). Presently, the most used antibody in our laboratory is anti-pan-neurofilament (a-PAN) antibody that, unlike other products, labels the large majority of nerve fibers. The detailed staining protocol follows. After deparaffination and rehydration with decreasing ethanol passages, nerve sections are incubated overnight in a solution containing anti-pan-neurofilament (a-PAN) primary antibody (polyclonal, rabbit, dilution 1:200, Sigma, St. Louis, MO). The sections are then washed in PBS and incubated for 1h in a solution containing CY3-conjugated anti-rabbit IgG (dilution 1:400, Dako, Milano, Italy) secondary antibody. They are finally mounted with a Dako fluorescent mounting medium. For confocal imaging of immunolabelled sections, we use a LSM 510 confocal laser microscopy system (Zeiss, Jena, Germany), which incorporates two lasers (Argon and HeNe) and is equipped with an inverted Axiovert 100M microscope. Confocal fluorescence images are usually taken using a 20x Plan-NEOFLUAR objective with a numerical aperture (NA) of 0.50 and a 40x Plan-NEOFLUAR objective with an NA of 0.75. An electronic zoom with a magnification ranging from 1 to 8 is employed to obtain further magnifications. To visualize fluorescence we use excitation from the 543-

nm HeNe laser line and emission passed through a high-pass (LP) 560 filter, which passes wavelengths greater than 560 nm to the detector.

In case of pre-embedding osmium tetroxide postfixation/staining, we have recently described a simple etching protocol to be carried out on nerve sections, which makes immunohistochemical analysis possible. Etching is obtained simply by incubating sections in H₂O₂ (Sigma, St. Louis, MO) (diluted 1:10 in distilled water) for 10 min after deparaffination and before primary antibody incubation.

Electron microscopy

After cutting, ultra-thin sections are placed on copper grids and stained with uranyl acetate and lead citrate. For our ultrastructural observations, we use a JEM-1010 transmission electron microscope (JEOL, Tokyo, Japan) equipped with a Mega-ViewIII digital camera and a Soft-Imaging System (SIS, Münster, Germany) for the computerized acquisition of the images. Ultrastructural observation can be done within a wide range of magnification. Technological advancements in electron microscopes (especially the employment of high resolution digital cameras to acquire images) allows today to analyse samples from very low (500x) up to very high (500,000) magnifications. The difference between peripheral nerves and of optic nerve is represented not only by the smaller fiber size in the optic nerve but also by the absence of connective tissue (collagen) typical of the CNS. Yet, a particular feature of the optic nerve is the absence of unmyelinated axons.

References

- Acar M, Karacalar A, Ayyildiz M, Unal B, Canan S, Agar E, Kaplan S. The effect of autogenous vein grafts on nerve repair with size discrepancy in rats: an electrophysiological and stereological analysis. *Brain Res* 2008; 1198:171-181.
- Amado S, Simões MJ, Armada da Silva PA, Luís AL, Shirosaki Y, Lopes MA, Santos JD, Fregnan F, Gambarotta G, Raimondo S, Fornaro M, Veloso AP, Varejão AS, Maurício AC, Geuna S. Use of hybrid chitosan membranes and N1E-115 cells for promoting nerve regeneration in an axonotmesis rat model. *Biomaterials* 2008; 29:4409-4419.
- Baryshnikova LM, Von Bohlen Und Halbach O, Kaplan S, Von Bartheld CS. Two distinct events, section compression and loss of particles ("lost caps"), contribute to z-axis distortion and bias in optical disector counting. *Microsc Res Tech* 2006;69:738-56.
- Battiston B, Tos P, Geuna S, Giacobini-Robecchi MG, Guglielmo R. Nerve repair by means of vein filled with muscle grafts. II. Morphological analysis of regeneration. *Microsurgery* 2000; 20:37-41
- Benes FM, Lange N. 2001. Two-dimensional versus three-dimensional cell counting: A practical perspective. *Trends Neurosci* 24:11-17.
- Canan S, Aktaş A, Ulkay MB, Colakoglu S, Ragbetli MC, Ayyildiz M, Geuna S, Kaplan S. Prenatally expose to a non-steroidal anti-inflammatory drug or saline solution impairs sciatic nerve morphology: A stereological and histological study. *Int J DevNeurosci*, 2008; 26:733-738.
- Campbell WW. 2008. Evaluation and management of peripheral nerve injury. *ClinNeurophysiol* 2008 119:1951-1965.
- Chalfoun CT, Wirth GA, Evans GRJ. Tissue engineered nerve constructs: where do we stand? *J Cell Mol Med* 2006; 10:309-317.
- Chen MB, Zhang F, Lineaweaver WC. Luminal fillers in nerve conduits for peripheral nerve repair. *Ann PlastSurg* 2006; 57:462-471.

- Cochran WG. 1977. Sampling techniques, 3rd ed. New York: John Wiley & Sons.
- Clavijo-Alvarez JA, Nguyen VT, Santiago LY, Doctor JS, Lee WP, Marra KG. Comparison of biodegradable conduits within aged rat sciatic nerve defects. *Plast Reconstr Surg* 2007; 119:1839-1851.
- Cruz Orive LM, Weibel ER. 1981. Sampling designs for stereology. *J Microsc* 122:235-257.
- Di Scipio F, Raimondo S, Tos P, Geuna S. A simple protocol for paraffin-embedded myelin sheath staining with osmium tetroxide for light microscope observation. *Microsc Res Tech* 2008; 71:497-502.
- Dykstra MJ. 1993. A Manual of Applied Techniques for Biological Electron Microscopy. Plenum Press, New York. 257 p.
- Fraher JP, O'Leary D, Moran MA, Cole M, King RH, Thomas PK. Relative growth and maturation of axon size and myelin thickness in the tibial nerve of the rat. I. Normal animals. *Acta Neuropathol* 1990; 79:364-374.
- Gardella D, Hatton WJ, Rind HB, Rosen GD, von Bartheld CS. 2003. Differential tissue shrinkage and compression in the z-axis: implications for optical disector counting in vibratome, plastic and cryosections. *J Neurosci Methods* 2003; 124:45-59.
- Geuna S. Appreciating the difference between design-based and model-based sampling strategies in quantitative morphology of the nervous system. *J Comp Neurol* 2000; 427:333-339.
- Geuna S, Tos P, Battiston B, Guglielmo R. Verification of the two-dimensional disector, a method for the unbiased estimation of density and number of myelinated nerve fibers in peripheral nerves. *Ann Anat* 2000; 182:23-34.
- Geuna S, Tos P, Guglielmo R, Battiston B, Giacobini-Robecchi MG. Methodological issues in size estimation of myelinated nerve fibers in peripheral nerves. *Anat Embryol* 2001; 204:1-10.
- Geuna S, Raimondo S, Nicolino S, Boux E, Fornaro M, Tos P, Battiston B, Perroteau I. Schwann-cell proliferation in muscle-vein combined conduits for bridging rat sciatic nerve defects. *J Reconstr Microsurg* 2003; 19:119-123.
- Geuna S, Tos P, Battiston B, Giacobini-Robecchi MG. Bridging peripheral nerve defects with muscle-vein combined guides. *Neurol Res* 2004a; 26:139-144.
- Geuna S, Gigo-Benato D, de Castro Rodrigues A. On sampling and sampling errors in histomorphometry of peripheral nerve fibers. *Microsurgery* 2004b; 24:72-76.
- Geuna S. The revolution of counting "tops": two decades of the disector principle in morphological research. *Microsc Res Tech* 2005; 66:270-274.
- Geuna S, Papalia I, Tos P. End-to-side (terminolateral) nerve regeneration: a challenge for neuroscientists coming from an intriguing nerve repair concept. *Brain Res Rev* 2006; 52: 381-388.
- Geuna S, Nicolino S, Raimondo S, Gambarotta G, Battiston B, Tos P, Perroteau I. 2007. Nerve regeneration along bioengineered scaffolds. *Microsurgery* 2007; 27:429-438.
- Geuna S, Raimondo S, Ronchi G, Di Scipio F, Tos P, Czaja K, Fornaro M. Histology of the peripheral nerve and changes occurring during nerve regeneration. *Int Rev Neurobiol* 2009; 87:27-46.
- Guillery RW. On counting and counting errors. *J Comp Neurol* 2002; 447:1-7.
- Gundersen HJG. Notes on the estimation of the numerical density of arbitrary profiles: the edge effect. *J Microsc* 1977; 111:219-223.
- Gundersen HJG. Estimators of the number of objects per area unbiased by edge effects. *Microsc Acta* 1978; 81:107-17.
- Gundersen HJG. Stereology of arbitrary particles. A review of unbiased number and size estimators and the presentation of some new ones, in memory of William R. Thompson. *J Microsc* 1986; 143:3-45.
- Hoffman PN. The synthesis, axonal transport, and phosphorylation of neurofilaments determine axonal caliber in myelinated nerve fibers. *Neuroscientist* 1995; 1:76-84
- Hoke A. Mechanisms of Disease: what factors limit the success of peripheral nerve regeneration in humans? *Nat Clin Pract Neurol* 2006; 2:448-454.
- Kanaya F, Firrell JC, Breidenbach WC. Sciatic function index, nerve conduction tests, muscle contraction, and axon morphometry as indicators of regeneration. *Plast Reconstr Surg* 1996; 98:1264-1271.
- Kaplan S, Geuna S, Ronchi G, Ulkay MB, von Bartheld CS. Calibration of the stereological estimation of the number of myelinated axons in the rat sciatic nerve: a multicenter study. *J. Neurosci. Methods* 2010; 187:90-9.
- Kaplan S, Pişkin A, Ayyıldız M, Aktaş A, Köksal B, Ulkay MB, Türkmen AP, Bakan F, Geuna S. The effect of melatonin and platelet gel on sciatic nerve repair: an electrophysiological and stereological study. *Microsurgery* 2011; 31:306-313.
- Keskin M, Akbaş H, Uysal OA, Canan S, Ayyıldız M, Ağar E, Kaplan S. Enhancement of nerve regeneration and orientation across a gap with a nerve graft within a vein conduit graft: a functional, stereological, and electrophysiological study. *Plast Reconstr Surg* 2004; 113:1372-9.
- Larsen JO. Stereology of nerve cross sections. *J Neurosci Meth* 1998; 85:107-118.
- Luís AL, Amado S, Geuna S, Rodrigues JM, Simões MJ, Santos JD, Fregnan F, Raimondo S, Veloso AP, Ferreira AJ, Armada-da-Silva PA, Varejão AS, Maurício AC. Long-term functional and morphological assessment of a standardized rat sciatic nerve crush injury with a non-serrated clamp. *J Neurosci Methods* 2007; 163:92-104.
- Lundborg G. Enhancing posttraumatic nerve regeneration. *J Periph Nerv Syst* 2002; 7:139-140
- Lundborg G. 2005. Nerve Injury and Repair, 2nd ed. Churchill Livingstone: Edinburgh.
- Mayhew TM, Gundersen HJ. If you assume, you can make an ass out of u and me: a decade of the disector for stereological counting of particles in 3D space. *J Anat* 1996; 188:1-15.
- Pakkenberg B, Gundersen HJ. Neocortical neuron number in humans: effect of sex and age. *J Comp Neurol* 1997; 384:312-320.
- Papalia I, Geuna S, Tos PL, Boux E, Battiston B, Stagno D'Alcontres F. Morphologic and functional study of rat median nerve repair by terminolateral neurotomy of the ulnar nerve. *J Reconstr Microsurg* 2003; 19:257-264.
- Papalia I, Cardaci A, d'Alcontres FS, Lee JM, Tos P, Geuna S. Selection of the donor nerve for end-to-side neurotomy. *J Neurosurg* 2007; 107:378-382.
- Pease DC. 1964. Histological techniques for electron microscopy. Academic Press, New York. 381 p.

- Raimondo S, Nicolino S, Tos P, Battiston B, Giacobini-Robecchi MG, Perroteau I, Geuna S. Schwann cell behavior after nerve repair by means of tissue-engineered muscle-vein combined guides. *J Comp Neurol* 2005; 489:249-259.
- Raimondo S, Fornaro M, Di Scipio F, Ronchi G, Giacobini-Robecchi MG, Geuna S. Methods and protocols in peripheral nerve regeneration experimental research: part II-morphological techniques. *Int. Rev. Neurobiol.* 2009;87:81-103.
- Raimondo S, Fornaro M, Tos P, Battiston B, Giacobini-Robecchi MG, Geuna S. Perspectives in regeneration and tissue engineering of peripheral nerves. *Ann Anat* 2011; 193:334-340.
- Roglio I, Giatti S, Pesaresi M, Bianchi R, Cavaletti G, Lauria G, Garcia-Segura LM, Melcangi RC. Neuroactive steroids and peripheral neuropathy. *Brain Res Rev* 2008; 57:460-469.
- Saper CB. Unbiased stereology: three-dimensional measurement in microscopy. *Trends Neurosci* 1999; 22:94-5.
- Schiønning JD, Larsen JO. A stereological study of dorsal root ganglion cells and nerve root fibers from rats treated with inorganic mercury. *Acta Neuropathol* 1997; 94:280-286
- Schmitz C, Hof PR. Design-based stereology in neuroscience. *Neuroscience* 2005;130:813-831.
- Sinis N, Schaller HE, Becker ST, Lanaras T, Schulte-Eversum C, Müller HW, Vonthein R, Rosner H, Haerle M. Cross-chest median nerve transfer: a new model for the evaluation of nerve regeneration across a 40 mm gap in the rat. *J Neurosci Methods* 2006; 156: 166-172.
- Sinis N, Schaller HE, Becker ST, Schlosshauer B, Doser M, Roesner H, Oberhoffner S, Müller HW, Haerle M. Long nerve gaps limit the regenerative potential of bioartificial nerve conduits filled with Schwann cells. *Restor. Neurol, Neurosci* 2007; 25:131-41.
- Sinis N, Guntinas-Lichius O, Irintchev A, Skouras E, Kuerten S, Pavlov SP, Schaller HE, Dunlop SA, Angelov DN. Manual stimulation of forearm muscles does not improve recovery of motor function after injury to a mixed peripheral nerve. *Exp Brain Res* 2008; 185:469-483.
- Smith TMF. 1994. Sample surveys 1975-1990: an age of reconciliation? *Int Stat Rev* 62:5-34.
- Tos P, Calcagni M, Gigo-Benato D, Boux E, Geuna S, Battiston B. Use of muscle-vein-combined Y-chambers for repair of multiple nerve lesions: experimental results. *Microsurgery* 2004; 24:459-464.
- Tos P, Battiston B, Nicolino S, Raimondo S, Fornaro M, Lee JM, Chirila L, Geuna S, Perroteau I. Comparison of fresh and predegenerated muscle-vein-combined guides for the repair of rat median nerve. *Microsurgery* 2007; 27:48-55.
- Unal B, Tan H, Orbak Z, Kiki I, Bilici M, Bilici N, Aslan H, Kaplan S. Morphological alterations produced by zinc deficiency in rat sciatic nerve: a histological, electron microscopic, and stereological study. *Brain Res* 2005; 1048:228-234.
- Vleggeert-Lankamp CL. The role of evaluation methods in the assessment of peripheral nerve regeneration through synthetic conduits: a systematic review. *J Neurosurg* 2007; 107:1168-1189.
- vonBartheld CS. 2002. Counting particles in tissue sections: Choices of methods and importance of calibration to minimize bias. *Histol Histopathol* 17:639-648.
- Ward TS, Rosen GD, von Bartheld CS. Optical disector counting in cryosections and vibratome sections underestimates particle numbers: effects of tissue quality. *Microsc Res Tech* 2008; 71:60-8.
- West MJ. Stereological methods for estimating the total number of neurons and synapses: Issues of precision and bias. *Trends Neurosci* 1999; 22:51-61.
- Williams P L. 'Gray's Anatomy.' Churchill livingstone: London.1999.